

# Fabrication of high quality ferromagnetic Josephson junctions

M. Weides,<sup>1</sup> K. Tillmann,<sup>2,3</sup> and H. Kohlstedt<sup>1,4</sup>

<sup>1</sup>CNI - Center of Nanoelectronic Systems for Information Technology,  
Research Centre Juelich, D-52425 Juelich, Germany\*

<sup>2</sup>Institute for Solid State Research, Research Centre Juelich, D-52425 Juelich, Germany

<sup>3</sup>Ernst Ruska-Centre for Microscopy and Spectroscopy with Electrons,  
Research Centre Juelich, D-52425 Juelich, Germany

<sup>4</sup>Department of Material Science and Engineering and Department of Physics, University of Berkeley, California 94720, USA

(Dated: September 6, 2018)

We present ferromagnetic Nb/Al<sub>2</sub>O<sub>3</sub>/Ni<sub>60</sub>Cu<sub>40</sub>/Nb Josephson junctions (SIFS) with an ultrathin Al<sub>2</sub>O<sub>3</sub> tunnel barrier. The junction fabrication was optimized regarding junction insulation and homogeneity of current transport. Using ion-beam-etching and anodic oxidation we defined and insulated the junction mesas. The additional 2 nm thin Cu layer below the ferromagnetic NiCu (SINFS) lowered interface roughness and ensured very homogeneous current transport. A high yield of junctional devices with  $j_c$  spreads less than 2% was obtained.

PACS numbers:

Keywords: Josephson Junctions,  $\pi$ -contact, Superconductor ferromagnet superconductor junctions

## INTRODUCTION

The realization of qubits for quantum computation attracts considerable interest. One approach is to use low  $T_c$  Niobium Josephson junctions (JJ) which utilize an ultrathin ferromagnetic layer to change the coupling of the two superconducting electrodes [1, 2]. Whether the junction is in the 0 or  $\pi$  coupled state depends on the properties of ferromagnetic layer and especially its thickness  $d_F$ . The coupling state can be determined by

$$I_c \propto \exp(-d_F/\xi_{F1}) \left| \cos \frac{d_F}{\xi_{F2}} + \frac{\xi_{F1}}{\xi_{F2}} \sin \frac{d_F}{\xi_{F2}} \right|$$

with characteristic decay  $\xi_{F1}$  and oscillation length  $\xi_{F2}$  [3]. Transition from 0 to  $\pi$  occurs at  $I_c(d_{F,0-\pi}) = 0$  when critical current  $I_c$  cancels out. Such JJs which can be realized either in an SFS [4, 5, 6, 7] or an SIFS [8] layer sequence (S: Superconductor, F: Ferromagnet, I: Insulator). In contrast to SFS junctions the area-resistance ( $R \times A$ ) product of SIFS structures can be tuned over orders of magnitude by using appropriate oxidation conditions for the tunnel barrier formation. High ( $R \times A$ ) products simplify the voltage readout.

The first step to realize a qubit is the formation of a semi-fluxon. Recent theoretical considerations predict semi-fluxons in SIFS junctions with a step-like ferromagnetic layer [9]. Exploiting such semifluxon for qubits systems [10] demands low spread of extrinsic and intrinsic parameters, e.g. junction area and current density.

## SAMPLES

The fabrication of SIFS multi-layers was performed in-situ by a computer-controlled Leybold Univex 450B magnetron sputtering system. Thermally oxidized 4-inch Si

wafer served as substrates. The wafers were clamped onto a water cooled Cu-block. First a 120 nm Nb bottom electrode and an 5 nm thick Al overlayer were deposited. Subsequently the aluminium was oxidized for 30 min in a separate chamber at an oxygen partial pressure ranging from 0.015 to 0.45 mbar. As ferromagnetic layer we deposited the diluted Ni<sub>60</sub>Cu<sub>40</sub> alloy ( $T_C = 225$ K), followed by a 40 nm Nb cap-layer. For realization of "wedge" shaped NiCu-layer (Fig. 1), the substrate and sputter target are shifted about half the substrate length. This facilitates the preparation of SIFS (and SINFS, N: normal metal) junctions with different F-layer thicknesses to avoid the inevitable run to run variations. In this way we prepared F-layers ranging between 1 and 15 nm.

The argon pressure during sputtering was  $7.0 \cdot 10^{-3}$  mbar for Nb and Al and  $4.2 \cdot 10^{-3}$  mbar for Cu and NiCu, respectively. The background pressure was  $5 \cdot 10^{-7}$  mbar. Niobium was deposited statically with 2.00 nm/s at a power density of 5 W/cm<sup>2</sup> and NiCu: 0.34 nm/s at 0.6 W/cm<sup>2</sup>, while Al and Cu were deposited during sample rotation and at much lower deposition rates to obtain very homogeneous and uniform films: Al: 0.05 nm/s and Cu: 0.1 nm/s, both at 1.9 W/cm<sup>2</sup>.

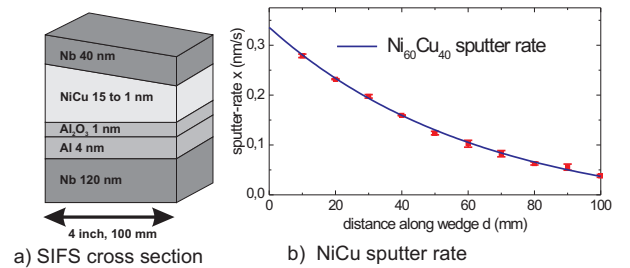


FIG. 1: (a) SIFS stack with "wedge"-shaped F-layer and (b) decreasing of the NiCu-sputter rates across a 4 inch wafer

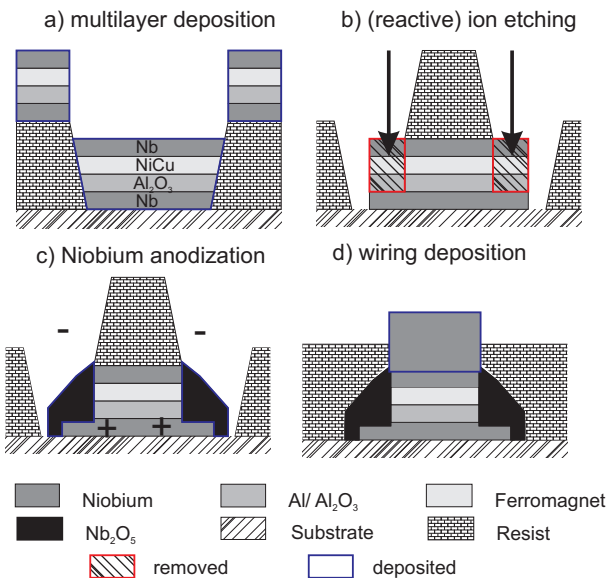


FIG. 2: (a) to (d) Three level photo mask procedure including ion-etching and Nb-anodization

### Patterning

Tunnel junctions with a crossbar geometry were patterned using optical lithography and Ar ion beam milling. A three level photo mask procedure was applied. First the bottom SIFS-layer areas were defined by a lift-off process. The situation after deposition of the SIFS sequence is shown in Fig. 2 (a).

After the lift-off various kinds of tunnel junctions were defined by applying the second photo mask step followed by reactive ion beam etching for the Nb layer and Ar for the NiCu and Al layers. The etching was controlled by a mass spectrometer and the procedure was stopped by reaching the  $\text{Al}_2\text{O}_3$  tunnel barrier (Fig. 2(b)). During etching the substrate was tilted by  $70^\circ$  and rotated to avoid etch fences at the edges of the mesas. The mesas were isolated by SNEAP (Selective Niobium Anodization Process) [11], Fig. 2(c).

It is interesting to note that the anodization was successful in the presence of NiCu layer. We obtained no problems with parallel currents through the NiCu layer during anodization. Probably the ferromagnetic layer is so thin that it is immediately overgrown by  $\text{Nb}_2\text{O}_5$  and  $\text{Al}_2\text{O}_3$  shortly after starting the anodization procedure. At a rate about 1 V/s we anodized the junction up to a voltage of 60 V (corresponding to 51 nm of anodized Niobium) was reached. The form factor of 2.3 for Niobium oxidation corresponds to 120 nm of formed  $\text{Nb}_2\text{O}_5$ , providing a complete side coverage of the barrier and the ferromagnetic layer.

In the last photo mask step the wiring layer was defined. After a slight ion beam etching to achieve low contact

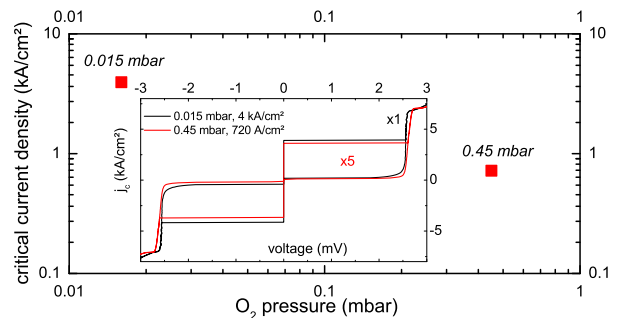


FIG. 3: SIS junctions with different oxidation conditions for the tunnel barrier forming.

resistance, a 300 nm thick Nb wiring was deposited. In Fig. 2 (d) the schematic cross-section of the device is shown.

To check the procedure standard SIS junctions were fabricated with areas between  $25 \mu\text{m}^2$  and  $1000 \mu\text{m}^2$ . In Fig. 3 two SIS characteristics are shown. For the ferromagnetic SIFS and SINFS junctions the areas were  $10.000 \mu\text{m}^2$  large.

### Oxidation

Besides a reliable junction patterning the interlayer roughness is essential for high quality ferromagnetic junctions. For SIFS junctions we optimized the  $\text{Al}_2\text{O}_3$  roughness as well as the roughness of the NiCu alloy to achieve low spreads of  $j_c$  from run to run. In this work we kept the oxidation time constant (30 min) and varied the oxygen pressure between 0.015 and 0.45 mbar. Using the very low oxidation pressure (0.015 mbar) we obtained current densities  $j_c$  of  $4 \text{ kA}/\text{cm}^2$  (Fig. 3) to counterbalance the strong Cooper-pair breaking in the ferromagnetic alloy, as seen in the  $I_c(d_F)$  dependence [12].

### SIFS and SINFS

On reference samples we performed ex-situ atomic force microscopy (AFM) measurements. The roughness of the  $\text{SiO}_2$  surface was less than 0.3 nm (rms). A 120 nm Nb film showed a roughness of 0.44 nm, which increased to 0.6 nm after deposition of 5 nm Al and even up to 0.9 nm after further 4 nm of NiCu. Insertion of a 2 nm Cu film after oxidation decreases the roughness of the SIN stack down to 0.50 nm. Now the top roughness of SIN (F: 4.7 nm) stack is about 0.68 nm. The ferromagnetic interlayer in a SINFS stack exhibited at both interfaces of NiCu a lower roughness than in a SIFS stack. Non-uniform growth of NiCu on top  $\text{Al}_2\text{O}_3$  may be caused by island-formation of the first monolayers when grown directly on  $\text{Al}_2\text{O}_3$ .

Fig. 4 displays a cross-sectional HRTEM (High-Resolution Transmission Electron Microscopy) image of a SIFS stack which was taken under bright atom contrast conditions using a spherical-aberration corrected electron microscope [13]. Because of the polycrystalline structure of the layers, individual nanocrystallites are not uniformly oriented with respect to the incident electron beam effecting that only certain lattice planes are resolved at atomic plane distances. Moreover, the image contrast is slightly bleary, which is most presumably due to both, the formation of amorphous interlayers during deposition and electron beam damage during operation of the instrument.

However, the basic layer structure becomes clearly visible from this image, i.e. the Al layer appears undulated, as opposed to a potential two-dimensionally flat layer. The lower Nb – Al and the upper NiCu – Nb interfaces show the very same undulations, meaning that roughness and interdiffusion occurs on a small length scale. Nonetheless the Al,  $\text{Al}_2\text{O}_3$  and NiCu layers are not directly distinguishable from each other in the micrograph. We attribute this observation to similar electron scattering amplitudes of the former materials and the interlayer roughness at rather small layer thicknesses, which may give rise to projection artefacts.

## RESULTS AND DISCUSSION

Our approach to patten ferromagnetic JJs differed from the standard procedure [4, 5, 6, 7, 8] where junction insulation is done by deposition of silicon-oxides after etching. The  $\text{Nb}_2\text{O}_5$  exhibits nearly defect free insulation between superconducting electrodes, even for thick (15 nm) ferromagnetic interlayers.

Electric transport measurements were made in a liq-



FIG. 4: Cross-sectional HRTEM image of a Nb/Al/NiCu/Nb stack

uid Helium dewar at 4.2 K. In Fig. 3 the current voltage characteristics for SIS junctions at different oxidation pressures are shown. The figures of merit  $V_m = I_c R$  (2mV), McCumber-Stewart parameter  $\beta_c = \frac{2eI_c R_n^2 C}{\hbar}$  and  $V_c = I_c R_n$  are for the  $j_c = 4 \text{ kA/cm}^2$  junction:  $V_m = 12 \text{ mV}$ ,  $\beta_c = 3.10$ ,  $V_c = 1.60 \text{ mV}$  and for the  $j_c = 720 \text{ kA/cm}^2$  junctions:  $V_m = 32.1 \text{ mV}$ ,  $\beta_c = 14.8$ ,  $V_c = 1.49 \text{ mV}$ . Larger  $j_c$  corresponded to inhomogeneous tunnel barrier formation, hence increased subgap leakage current and a decreased energy gap (inset of figure 3). Still these higher  $j_c$  junctions exhibit good junction parameters, so we used their tunnel barrier oxidation conditions (0.015 mbar) for the fabrication of SINFS stacks.

The Fraunhofer modulation of  $I_c$  is seen in Fig. 5 for SIFS junctions with 2 nm (a) and 4 nm (b) NiCu layers and a SINFS junction with 2nm Cu and 4.7nm NiCu (c). All the ferromagnetic junction investigated in this work are still in 0 coupled regime [12]. In general the interface barrier roughness leads to inhomogeneous current transport, which can cancel out the coherent Josephson coupling and leads to disturbed Fraunhofer pattern. The conditions for non-uniform supercurrent are given by the ratio of NiCu interface roughness over the decay length  $\xi_{F1}$  and oscillation length  $\xi_{F2}$  of the supercurrent. In  $\text{Ni}_{60}\text{Cu}_{40}$  these values are about 1 – 3 nm, to be published in [12].

For thin (below 3 nm) NiCu layers we see a clean Fraunhofer modulation (Fig. 5 (a)). However for thicker NiCu layers the  $I_c(H)$  deviated considerably (Fig. 5 (b)). Although electrical measurements on SIS junctions suggested a high quality barrier (inset of Fig. 3), this suggests some finite roughness of the  $\text{Al}_2\text{O}_3$  tunnel barrier and/or of the NiCu layer. As AFM-measurements indicated the 2nm NiCu layer on-top the  $\text{Al}_2\text{O}_3$  forms similar roughness contours, so effective thickness of NiCu is con-

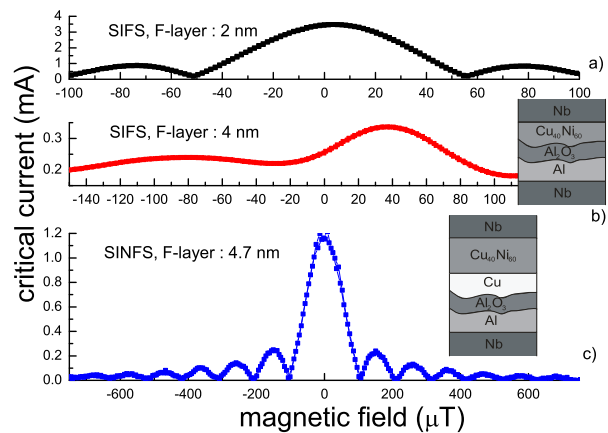


FIG. 5:  $I_c(H)$  of (a) SIFS (2 nm NiCu), (b) SIFS (4 nm NiCu) and (c) SINFS (Cu 2 nm, NiCu 4.7 nm) stack. Oxygen pressure is 0.45 mbar for SIFS and 0.015 mbar for SINFS type.

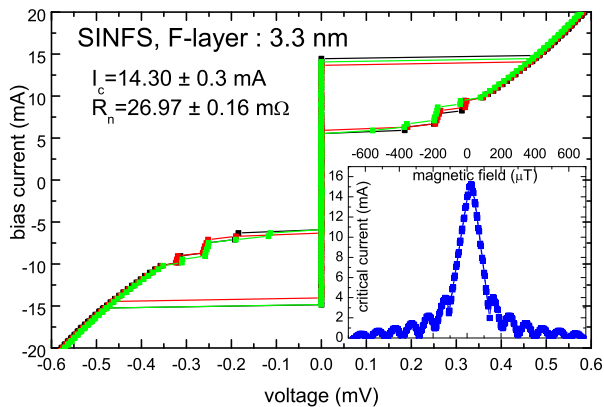


FIG. 6: IVs of three SINFS junction,  $O_2$  oxidation pressure is 0.015 mbar.  $\delta I_c = 2\%$ ,  $\delta R_n = 0.5\%$

stant and super-current transport remains homogeneous as seen in Fig. 5 (a). When doubling the thickness of NiCu to 4.7 nm its top roughness is about 0.9 nm and the effective NiCu layer thickness is not uniform. This is supported by transport measurements seen in Fig. 5 (b). By including a 2 nm Cu layer under the NiCu the  $I_c(H)$  we recovered the clean Fraunhofer pattern. We could even use the thinner  $Al_2O_3$  barrier for SINFS, although this should increase the  $Al_2O_3$  roughness slightly. The Cu-layer between  $Al_2O_3$  and NiCu smoothes the lower NiCu-interface and provides a uniform effective ferromagnetic layer. Even for thicker (up to 8.5 nm) NiCu-layers we see uniform supercurrents through such SINFS junctions (fig. 5 (c)). For NiCu thicker than 8.5 nm we can not measure any supercurrent due to the strong Cooper pair breaking. This will be reported elsewhere [12].

The strong proximity effect of Cu leads to weak pair breaking of the super-current in the N-layer. SIFS and SINFS samples (N: 2 nm Cu layer) showed identical critical current densities, so junction properties are determined by the ferromagnetic layer. For all NiCu thicknesses we obtained a low junction to junction deviation. In Fig. 6 the characteristics of three under-damped SINFS junctions with a 3.3 nm NiCu layer are shown. The parameter spread of critical current and normal re-

sistance (and therefore  $\beta_c$ ) is below 2% ( $I_c = 14,3$  mA,  $R_n = 26.97$  m $\Omega$  and  $\beta_c = 5.0$ ). Even the very sensitive sub-gap characteristics are nearly identical for all junctions as seen in Fig. 6. These junction exhibit a high-quality  $I_c(H)$  pattern (inset of Fig. 6), just like the Fraunhofer pattern of SINFS with 4.7 nm NiCu layer in Fig. 5 (c).

## CONCLUSION

Motivated by the demand for ferromagnetic JJ with low parameter spread, we have developed an alternative fabrication process. Transport measurements on SINFS junction showed that the quality of junctions was considerable improved using  $Nb_2O_5$  as insulator and planarization of the ferromagnetic interlayer by an additional Cu layer. Our fabrication procedure may offer a solution for the strict uniformity requirements for the formation of qubits.

---

\* Electronic address: m.weides@fz-juelich.de

- [1] A. Buzdin, JETP Lett. 78 (2003) 583–586.
- [2] E. A. Demler, G. B. Arnold, M. R. Beasley, Phys. Rev. B 55 (1997) 15174–15182.
- [3] A. Buzdin, Rev. Mod. Phys. 77 (2005) 935.
- [4] V. V. Ryazanov, V. A. Oboznov, A. Y. Rusanov, et al., Phys. Rev. Lett. 86 (2001) 2427–2430.
- [5] H. Sellier, C. Baraduc, F. Lefloch, et al., Phys. Rev. B 68 (2003) 054531.
- [6] Y. Blum, A. Tsukernik, M. Karpovski, et al., Phys. Rev. B 70 (2004) 214501.
- [7] C. Surgers, T. Hoss, C. Schonenberger, et al., J. Magn. Magn. Mater. 240 (2002) 598–600.
- [8] T. Kontos, M. Aprili, J. Lesueur, et al., Phys. Rev. Lett. 89 (2002) 137007.
- [9] E. Goldobin, D. Koelle, R. Kleiner, Phys. Rev. B 66 (2002) 100508.
- [10] E. Goldobin, K. Vogel, O. Crasser, R. Walser, W. Schleich, D. Koelle, R. Kleiner, Phys. Rev. B 72 (2005) 054527.
- [11] M. Gurvitch, M. A. Washington, H. A. Huggins, et al., IEEE Transactions on Magnetics 19 (1983) 791–794.
- [12] Weides, Kohlstedt, paper in preparation.
- [13] M. Lentzen, B. Jahnen, C. L. Jia, A. Thust, K. Tillmann, K. Urban, Ultramicroscopy 92 (2002) 233–242.